EXPLICIT FORMULATION FOR THREE-DIMENSIONAL CICLIC ANALYSIS OF R.C. STRUCTURES

L. SGAMBI

Ph.D. Student, Department of Structural and Geotechnical Engineering,
University ''La Sapienza'' Rome, Italy
sgambi.luca@libero.it

ABSTRACT

Scope of this work is the definition of a material law able to represent the behavior of three-dimensional reinforced concrete structures subjected to cyclical load histories. Resuming the hypotheses presented in literature, as in the publications of Vecchio, who considers a orthotropic material law in both phases of loading and unloading, it has been formulated and implemented a constitutive model suitable to analysis based on explicit algorithms. The consideration of orthotropic tensional field during loading, unloading and reloading, places remarkable problems, both from theoretical and numerical points of view, because during the load history, it varies the value of the damage along a principal direction and also the principal orientation. Being the law formulated based on CFT and MCFT models class, the total answer is calculated in function of the uniaxial law, that is thought valid along each of the three principal directions. In this way, fundamental importance assumes the single uniaxial law and, of course, also the laws that govern the load and the unload of the material in three-dimensional space. In order to validate the material formulation, it has been analyzed one reinforced concrete wall loaded to remarkable cyclical shear tension.

1. INTRODUCTION

In the reinforced concrete (R.C.) structures, the analysis that we can use are based on very numerous different material modeling, some founded on fracture mechanics, some founded on non linear elastic models, and so on. Different models are based on discrete fissure, other on diffuse fissure; besides, a kind of fissure can be rotating or fixed.

In this way, for monotonic load, the behavior of R.C. structures is today reproduced by a great number of models. Instead, the models able to describe the behavior of generic R.C. structures subject to cyclic load are more complex and therefore not so numerous in literature, especially when the cyclic load can change the sign.

The complex behavior of reinforced concrete subjected to cyclic load requires the necessity to introduce a simplyficative hypothesis to achieve some valid result in really interesting engineering structures.

Many models reported in literature consider an orthotropic constitutive law during the phase of load, but an isotropic constitutive law during the phases of unload or reload. The material orthotropy is a very important characteristic on the R.C. structures analysis, especially if the structures have a great shear stress. To consider an orthotropic stress state during all the phases of the load history, one meets remarkable theoretical and numerical problems, because during the phases, it changes the quantity that defines the damage state and, also, the orientation of the principal direction.

Resuming the hypothesis presented in literature, notably established by Vecchio [8]-[9], to consider the orthotropy during the loading, the unloading and the reloading phase, a constitutive law has been formulated and implemented in one user subroutine for the commercial code ABAQUS/EXPLICIT. This constitutive law is suitable to analyze a three-dimensional R.C. structure subject to a generic history load. The formulation is founded essentially on the CFT and MCFT models [8] and therefore the global response is calculated with reference to the responses in the principal directions. It follows that the uniaxial law and the algorithm of analysis for the material unload and reload, assume great importance.

2. THE UNIAXIAL LAW

One can consider that uniaxial law is composed of three parts:

- the envelope law,
- the unload-reload law,
- the residual deformation law.

We assume that the envelope curve is equal to the uniaxial law. If the kind of deformation is a compression state, we can adopt the following expression:

$$\sigma_i = \begin{cases} \sigma_p \cdot \dfrac{\varepsilon}{\varepsilon_0} \cdot \left(2 \cdot - \dfrac{\varepsilon}{\varepsilon_0} \right) & if \quad \varepsilon > 2 \cdot \varepsilon_0 \\ 0 & if \quad \varepsilon < 2 \cdot \varepsilon_0 \end{cases} \tag{1}$$

where ε_0 is the deformation corresponding to the greatest stress value in the parabolic law.

In case of tension, the envelope law is:

$$\sigma_i = \begin{cases} E_0 \cdot \varepsilon_i & if \quad \varepsilon_i < \varepsilon_{cr} \\ \dfrac{E_0 \cdot \varepsilon_{cr}}{1 + \sqrt{500 \cdot \varepsilon_i}} & if \quad \varepsilon_i > \varepsilon_{cr} \end{cases} \tag{2}$$

where ε_{cr} is the concrete cracking deformation (for default, assumed equal to *0.00008*).

We can note that these expressions aren't fixed but, in case of necessity, one can replace them with other ones more appropriate. During the cyclic analysis, the concrete behavior does not remain on the envelope curve, because of an unload branch. The expression used to describe the curve, unload-reload phase in compression, is the following:

$$\sigma_i = \begin{cases} 0 & if \quad \varepsilon_{ci} > \varepsilon^r_{ci} \\ (\varepsilon_{ci} - \varepsilon^r_{ci}) \cdot \dfrac{\sigma_{cim}}{\varepsilon_{cim} - \varepsilon^r_{ci}} & if \quad \varepsilon^r_{ci} > \varepsilon_{ci} > \varepsilon_{cim} \end{cases} \tag{3}$$

where ε^r_{ci} is the residual compression deformation and ε_{cim} is the greatest deformation along the direction examined. One can note that the unload-reload law in compression state is simply formed by two lines that join the point (*0,0*) with the point ($0,\varepsilon^r_{ci}$) and the point ($0,\varepsilon^r_{ci}$) with the point ($\sigma_{cim},\varepsilon_{cim}$).

If the cyclic behavior is in the tension state, one assumes the following secant law:

$$\sigma_i = \frac{\varepsilon_{ti} \cdot \sigma_{tim}}{\varepsilon_{tim}} \tag{4}$$

that represents a line that join the point ($\sigma_{tim},\varepsilon_{ti}$) with the point (*0,0*).

In all the previous expressions, some symbols of deformation have an index *m*, meaning in this case that this is the greatest value of the correspondent deformation reached during the previous load history. The corresponding stress component (that has again the index *m*) is calculated by the envelope law: in three dimensional problem, however, one cannot consider only the greatest value previously reached, but it is also necessary to consider the directions along which this deformation has been taken.

The implemented model considers a residual deformation in the compression state only. The value of the deformation is calculated when the representative point (ε_i,σ_i) is on the envelope law, and is calculated considering the following expression:

$$\varepsilon_r = \varepsilon_m - \frac{\sigma_I}{E_0} \tag{5}$$

Due to the fact that the envelope tension is univocally defined in correspondence of the current greatest deformation (ε_{cim}), the residual deformation is also univocal.

3. LOADING AND RELOADING HIPOTESYS

Due to the fact that the problem is three-dimensional, it is not straightforward to consider the orthotropy during the unload and reload branch. In particular, it is not sufficient to save the value of the greatest deformations only, but it is also necessary to save the information related to the directions where these deformations are developed.

The control of the unload and reload for the tension state are executed updating, for each step, a tensor of the greatest tension deformations and a tensor of residual compression deformations. These tensors are saved in the global coordinates system, but the updating is executed in the current principal system. Therefore, for each load history step, the principal directions are calculated and both the tensors are rotated in the current principal system and, if it is necessary, the diagonal terms are updated. After the update, the tensors are rotated in the global coordinates system and saved. With these informations and with a series of algorithms reported in [3] it is possible to decide if the principal tensions must be calculated through an envelope law or an unload - reload law.

4. THE FAILURE SURFACE

The first problem analyzed is the capacity to reproduce the bi-axial concrete failure surface. Kupfer and Gerstle obtained the well-known experimental curve in 1973 [4]. The load histories considered are the following:

History 1	Monotonic radial load
History 2	Monotonic non radial load
History 3	Monotonic non radial load
History 4	Monotonic non radial load
History 5	Non radial load with unload
History 6	Non radial load with unload and reload

The diagram interpolating the ultimate tension and deformation is showed in figure 1 (the stars are the rupture points). The surface appears closed and convex, and reproduces approximately the experimental surface.

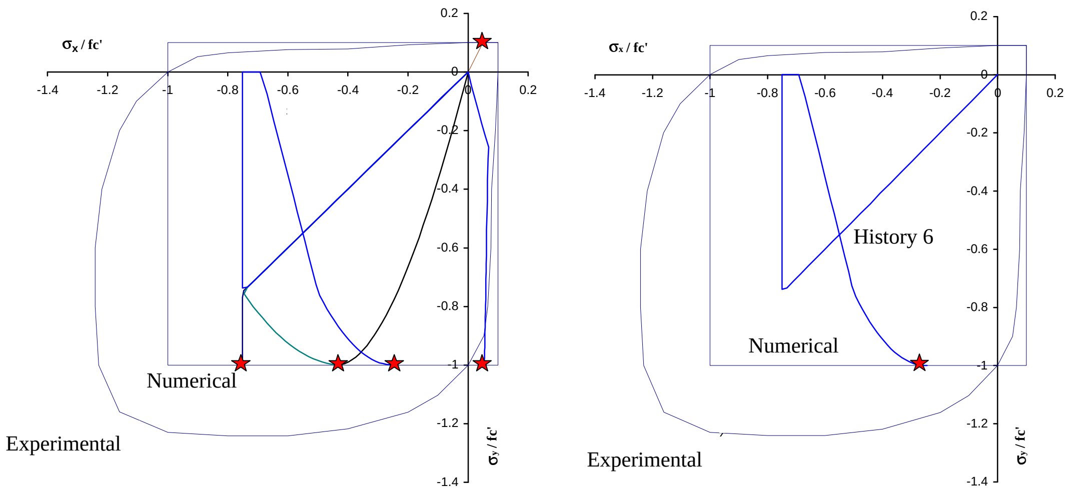

Figure 1: Failure diagram of Kupfer – Gerstle and history of load number six.

In figure 1 is also showed the history load number 6: this history presents one complete cycle of load, unload and reload in the Y direction, but only load and unload cycles in the X direction.

Another important failure surface is the one denoted as the Bresler-Pister diagram. This surface, experimentally obtained for the first time in 1958, is formed by the rupture point in the $\tau - \sigma$ domain.

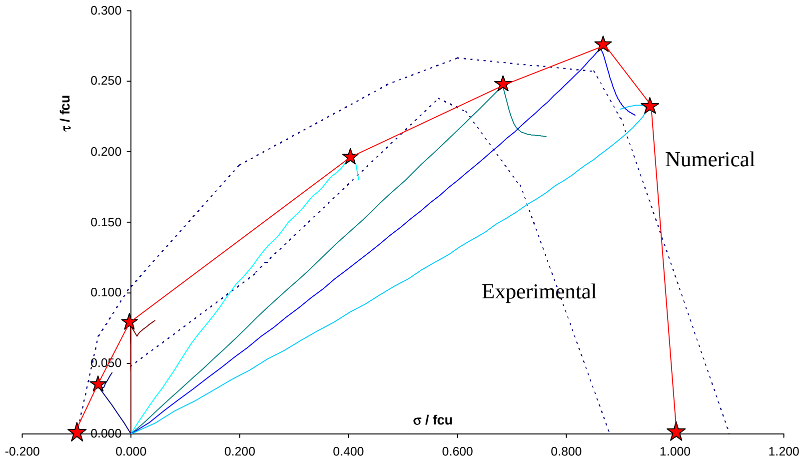

Figure 2: Failure diagram of Bresler - Pister.

To reproduce this diagram, one considers six different shear-normal stress histories. The curve obtained by the proposed formulation is still close to the experimental surface.

5. PANEL SUBJECTED TO SHEAR-COMPRESSION CICLIC LOAD HISTORY

In this numerical elaboration, one has analyzed the response of the proposed model when the concrete is subject to a generic history load. These panels belong to an experimental work executed by the University of Toronto (Canada), with the purpose to gather a numerous experimental data base to confirm the numerical models.

One has considered three panels (PDV1, PDV2, and PDV3) with dimensions *890x890x70* mm, and with orthogonal reinforcing steel layer. The mechanical characteristics of the concrete are different for each panel, but are characterized by common use values ($f_c' = 26.6 - 23.7 - 34.1$ *Mpa*).

The characteristics of steel are, instead, equal for all the panels and specifically: horizontal reinforcement $r_x = 1.82\%$ with yield tension of $f_{yx} = 282$ *MPa*, vertical reinforcement $r_y = 0.91\%$ and $f_{yy} = 282$ *MPa*.

All the panels are subject to a bi-axial history load of shear and compression, where the value of the loads respect the following ratio: $f_{nx}; f_{ny}; n = -0.4; -0.4; 1.0$. Finally, the panel PDV1 is subject to monotonic load history; the panel PDV3 is subject to unidirectional cyclic history (no sign inversion); the panel PDV2 is subject to shear cyclic history (with sign inversion).

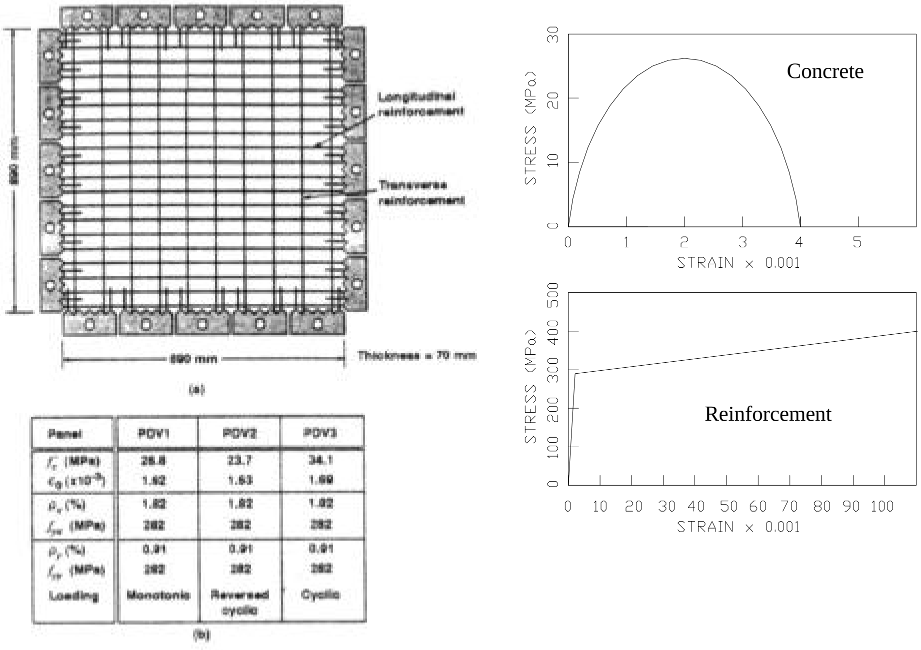

Panel	PDV1	PDV2	PDV3
f'_c (MPa)	26.8	23.7	34.1
ϵ_0 ($\times10^{-3}$)	1.62	1.63	1.69
ρ_x (%)	1.82	1.82	1.82
f_{yx} (MPa)	282	282	282
ρ_y (%)	0.91	0.91	0.91
f_{yy} (MPa)	282	282	282
Loading	Monotonic	Reversed cyclic	Cyclic

Figure 3: Geometries and mechanical characteristics for the tree panels [9].

The panel PDV1 is subject to a monotonic load history: the force of shear and the force of compression always increase.

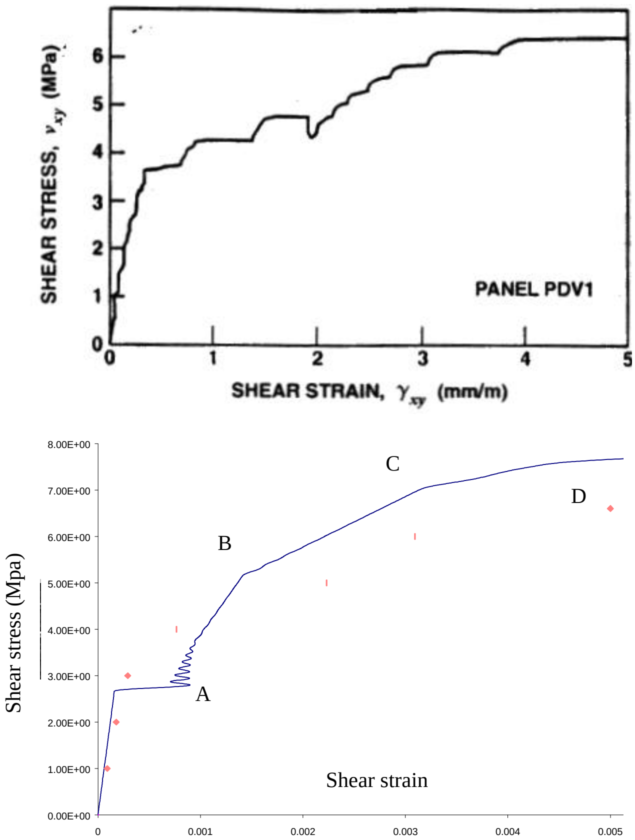

Figure 4: Experimental and numerical responses for the panel PDV1.

In figure 4 are showed both the experimental and the numerical responses. The numerical response is very similar to the experimental curve, denoting for the model a good behavior in presence of monotonic load. In figure 4, one can put in evidence a first line approximately linear, a sudden horizontal jump indicator of the concrete cracking, and a sequence of the linear line. These lines join in the points A, B, C and D; the point B and C are representative of the reinforced yielding (horizontal and vertical). After point C, the panel has still a small stiffness because, for the steel reinforcement, one has assumed a hardening behavior. However the panel crashes early (point D).

It's important the behavior of the model in the point A. This point represents the beginning of the cracking process, that is connected with the attainment of the greatest tension stress. When the concrete cracks, the explicit algorithm used by ABAQUS/EXPLICIT introduces the dynamic behavior that one can observe because, for one moment, the panel doesn't have a positive stiffness. However, the stress reaches early the reinforcement steel and the stiffness returns positive. This is the reason of the oscillations visible near the point A: these oscillations vanish soon, because one has assumed a very long time for the numeric history. In this manner the result isn't influenced from the dynamic behavior and the numeric result can be confrontable with experimental curves (obtained with a static load). In conclusions, the results for the panel PDV1 seem good.

The panel PDV2 is subject to shear cyclic history with sign inversion. In figure 5 are showed the experimental and the numerical responses. The comparison between the two curves is acceptable.

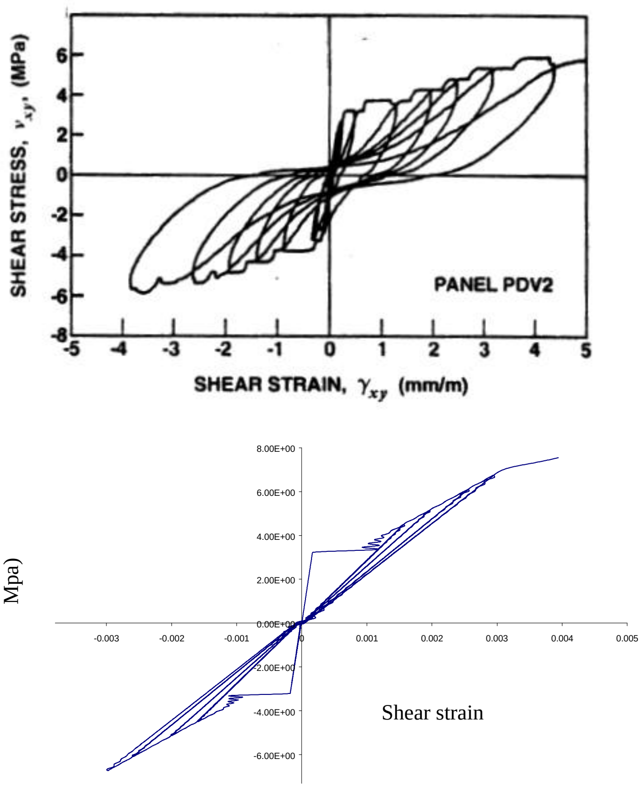

Figure 5: Experimental and numerical responses for the panel PDV2.

Also in this case, one can put in evidence the oscillations caused by the concrete cracking.

The inversion of the load and the inversion of the stress sign cause some light oscillations that do not influence so much the results. These are fairly good and, in particular, the model is able to consider the material orthotropy during all the phases, loading, unloading and reloading.

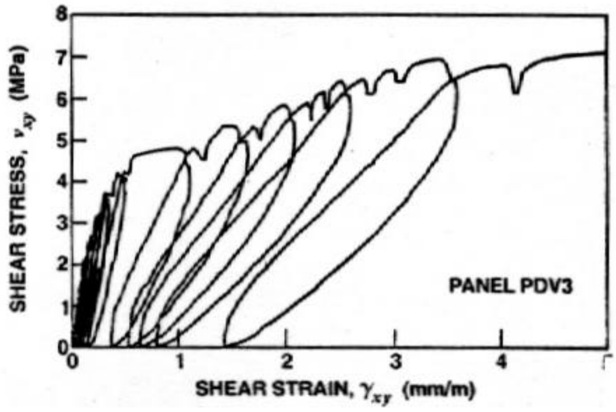

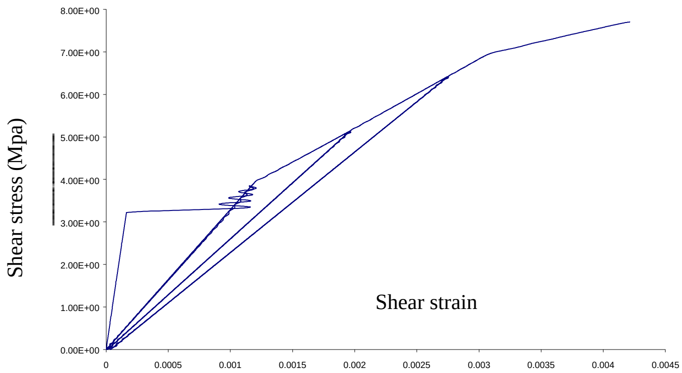

Figure 6: Experimental and numerical responses for the panel PDV3.

The panel PDV3 is subject to cyclic history but without sign inversion.

In figure 6 are showed the experimental and the numerical responses. The comparison between the two curves is acceptable, even if the residual deformations are less than the ones measured experimentally.

6. A SHEAR WALL ANALYSIS

The final case examined to validate the implemented model, is the analysis of a shear wall. This structure belongs to an experimental work reported in [6]. The wall examined is named "wall B2" and is *1910 mm* wide and *4570 mm* high. The thickness is *102 mm* in the center of the wall, and *305 mm* at the edge. A complete description of the wall geometry is reported in figure 7.

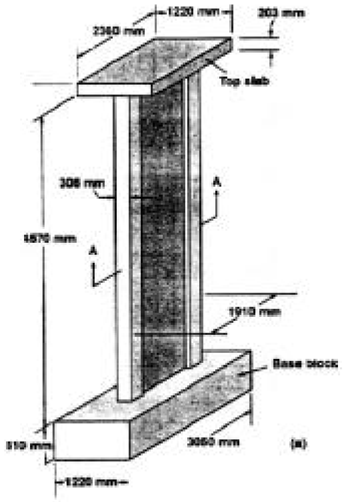

Zone	Horizontal reinforcemet		Vertical reinforcement	
	%	fy	%	fy
Top slab	0.63	533	0.29	533
Web	0.63	533	3.67	410
Edge	3	600	3	600

Figure 7: Geometry and mechanics characteristics of the Wall B2.

This wall is subject to a shear force at the top. This analysis is a severe trial to validate the model because the wall has a great diffusion zone and reach a big shear stress value. The cyclic deformation causes a continue rotation of all tensors introduced to describe the cyclic behavior and, for this reason, this test permits to examine the validity of the hypothesis previously introduced.

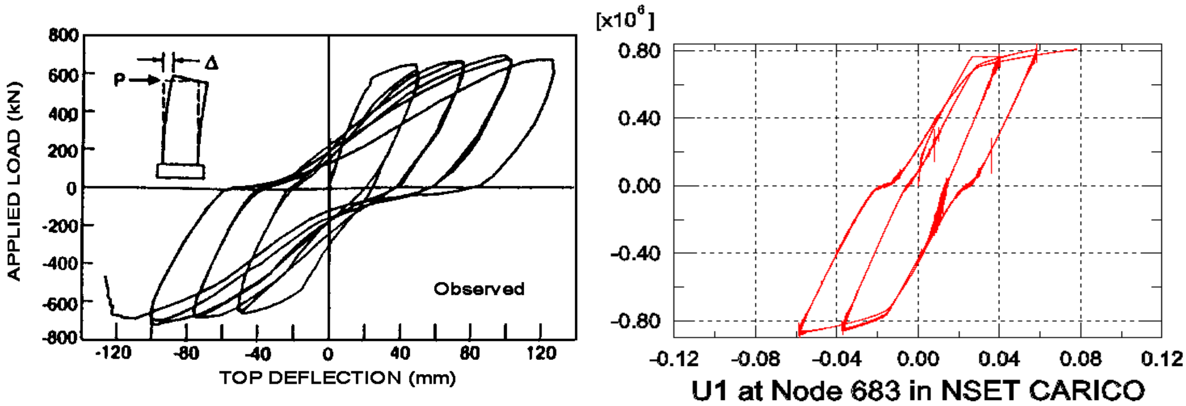

Figure 8: Experimental and numerical responses for the wall B2.

The numerical elaboration has been developed until the second cycle. The accuracy of the response is already evident: the maximum load is nearly equal to the experimental results and the general behavior during the cyclic load appear good.

In figure 9 is showed the cracking zone evolution during the history load, where the gray indicates the zones with great cracks and the red those with little cracks.

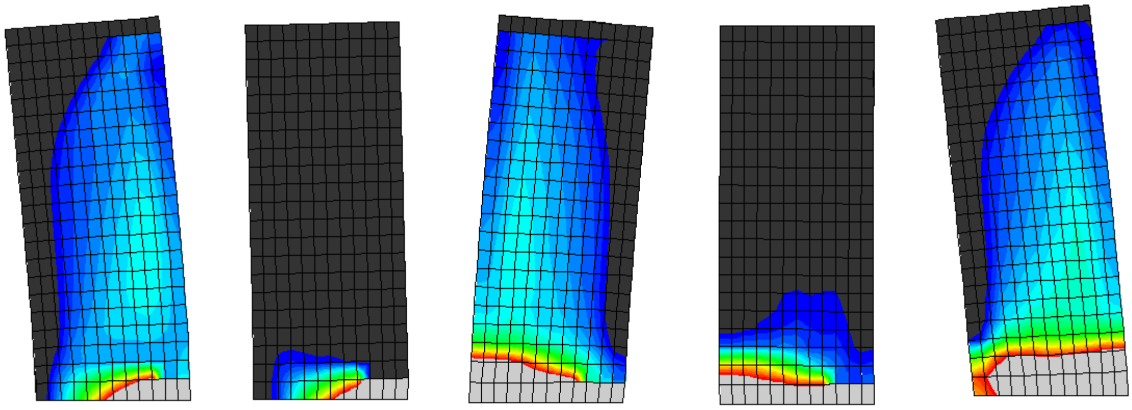

Figure 9: Evolution of the crack zone during the history load.

From figure 9 we can note the cracks pattern evolution, in particular the opening and the closing of the cracks during the load cyclic history.

7. BIBLIOGRAPHY

[1] Biondini F. : Strutture da ponte soggette ad azioni di tipo sismico. Modellazione ed ottimizzazione, *Tesi di Dottorato*, Politecnico di Milano (2000).

[2] Bontempi F, Malerba P. G., Romano L. : Il modello MCFT nell'analisi per elementi finiti di strutture piane in C.A., *Studi e ricerche*, Politecnico di Milano (1994).

[3] Chillé F., Frigerio A., : Sviluppo e implementazione di un legame costitutivo con formulazione esplicita per analisi di strutture in cemento armato tridimensionali soggette a storie di carico generiche, *ENEL.Hydro – PIS*, Milano (2001).

[4] Kupfer, Gerstle, : Behaviour of concrete under biaxial stresses, *J. of the Engineering Mechanics Division*, (1973).

[5] Malerba P. G., : Analisi limite e non lineare di strutture in cemento armato, *CISM* Udine, (1998).

[6] Oesterle : Earthquake-Resistant structural walls – Tests of isolated walls, *Report to the National Science Foundation*, Construction Technology Laboratories, Portland Cement Association, Skokie, Nov. (1976)

[7] Sgambi L. : Modellazione 3D di strutture in C.A. e C.A.P. in campo non lineare, *Tesi di Specializzazione*, Scuola "F.lli Pesenti", Politecnico di Milano (2001).

[8] Vecchio F. J. : Non linear Finite Element Analysis of Reinforced Concrete Membranes, *ACI Structural Journal* (1989).

[9] Vecchio F. J. : Towards cyclic load modeling of reinforced concrete, *ACI Structural Journal* (1999).